to Mn(IV) bound on one side of the porphyrin ring. Such a formulation would also agree with the large exchange coupling observed from magnetic susceptibility measurement: known Mn(III)/Mn(IV) pairs bridged by oxygen atoms are strongly coupled. A large gap between the ground state $S = {}^1/_2$ and the first excited state $S = {}^3/_2$ is also consistent with a slow relaxation rate allowing the observation of the EPR signal of dimer 1 at 110 K (we would like to stress that the signal of dimer 2 can also be observed at the same temperature).[37] Dimer 1 must be different from the [TPPMn^{III}-O-Mn^{IV}-TPP]-X observed in ref 35 since the EPR spectra are different (signal width 1070 G). This difference is also expected from redox behavior, dimer 1 being reduced at a very negative potential. A possible structure would be

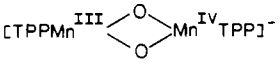

This complex could be related to the peroxo-bridged species [TPPMn^{II}-O_2-Mn^{III}TPP]$^-$, postulated in ref 22, by a change in the geometry and oxidation level of the bridge. The value $a_{Mn(IV)}$ = 81 G close to the one of asymmetrical Mn(IV) monomer could be in agreement with our hypothesis. The equilibrium

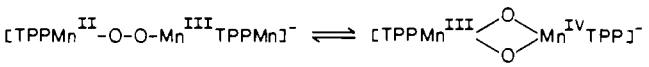

could exist. Consequently, the following mechanism is proposed:

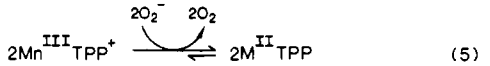

(5)

$$Mn^{II}TPP + O_2^{\bullet-} \rightleftharpoons [Mn^{III}TPPO_2]^- \quad (6)$$

$$[Mn^{III}TPPO_2]^- + Mn^{II}TPP \rightleftharpoons [TPPMn^{II}\text{-}O\text{-}O\text{-}Mn^{III}TPP]^- \quad (7)$$

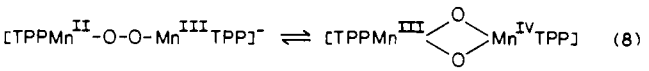

(8)

(37) Chang, H. S.; Larsen, S. K.; Boyd, P. D. W.; Pierpont, C. G.; Hendrickson, D. N. *J. Am. Chem. Soc.* **1988**, *110*, 4565.

[$Mn^{III}TPPO_2$]$^-$ and [TPPMn^{II}-O-O-Mn^{III}TPP]$^-$ or

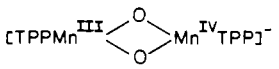

would be the species reduced at the dropping mercury electrode with one electron and two electrons, respectively, at the same half-wave potentials: −1.28 and −1.45 V. The fact that [$Mn^{III}TPPO_2$]$^-$ is reduced at the same potential as $Mn^{II}TPP$ is strong evidence that $O_2^{\bullet-}$ does not strongly bind to $Mn^{II}TPP$ in coordinating solvents (DMSO or DMF). Equation 5 is supported by polarography, visible spectroscopy, and EPR spectroscopy, though we failed electrochemically to give absolute evidence for O_2 formation. With $Mn^{II}TPP$ as the starting material, two situations can occur: with less than 1 equiv of superoxide ion, the above mechanism is valid starting from eq 6; with 1 equiv or a slight excess of superoxide, all the $Mn^{II}TPP$ is converted into [$Mn^{III}TPPO_2$]$^-$ and the reaction cannot go further. The effect of adding dioxygen in DMSO solutions can be so interpreted: dioxygen may partly cause the decomposition of [$Mn^{III}TPPO_2$]$^-$, which proves to be not very stable in DMSO (vide supra), into the $Mn^{II}TPP$ necessary for the reaction to proceed (eq 7). A reviewer suggested to us that the initiation of dimer formation could be provoked by further reduction of Mn(II) to Mn(II)$^-$, which then would react rapidly with the $O_2^{\bullet-}$ in the diffusion layer. This is consistent with the first reduction wave at −1.28 V, the dimer being reduced once further at −1.45 V. This is a possible notion, consistent with the reversible cyclic voltammetry, but we could not get evidence for it: Coulometric experiments performed at those potentials to identify the reduction products produced at the electrode induced decomposition of the porphyrin.

The mixed-valence dimeric manganese porphyrin we identified did not prove stable enough to be isolated. In solution, it slowly decomposes to $Mn^{II}TPP$. So it may be possible that, like [Mn-$TPPO_2$]$^-$, it plays a role in the manganese porphyrin catalyzed oxidation by dioxygen. Moreover, we have detected its formation by EPR spectroscopy in the oxidation reaction of 2,4,6-tri-*tert*-butylphenol by $Mn^{II}TPP$ and dioxygen, in toluene or CH_2Cl_2.

Acknowledgment. We gratefully acknowledge Dr. J. Huet (Laboratoire de Chimie Bioorganique et Bioinorganique), who recorded the first EPR spectra.

Contribution from the Department of Chemistry, University of California, Berkeley, California 94720

Isomerization and Solution Structures of Desferrioxamine B Complexes of Al^{3+} and Ga^{3+} [1]

Brandan Borgias, Alain D. Hugi, and Kenneth N. Raymond*

Received August 26, 1988

The Ga(III) and Al(III) complexes of desferrioxamine B (H_4DFO^+) have been prepared and purified by cation-exchange liquid chromatography. Both complexes elute as single bands, with elution rates comparable to those measured for the trans isomer(s) of the kinetically inert Cr(HDFO)$^+$ complex. The solution thermodynamics of Ga(HDFO)$^+$ show that the cationic complex is the only significant species from pH 2 to pH 9. Above pH 9 the complex undergoes hydrolysis. Its stability constant, log K_{ML}, is 27.56 (compared to 30.60 for Fe(III)). The NMR spectra of both the Ga and Al complexes indicate the presence of two isomers in solution, whose rapid interconversion prevents chromatographic separation. The kinetics of isomerization of Ga(HDFO)$^+$ were studied by variable-temperature ^{13}C measurements in D_2O, methanol-d_4, and dimethyl-d_6 sulfoxide. The following kinetic parameters were obtained at 25 °C: k (s^{-1}), $\Delta H^{\ddagger}$ (kcal·mol^{-1}) and $\Delta S^{\ddagger}$ (cal·mol^{-1}·K^{-1}): 13 (1), 13 (1), and −10 (3) in water; 73 (7), 17 (2), and +8 (8) in methanol; 4.1 (6) × 10^2, 17 (5), and +10 (15) in DMSO. These results, and the observation that in water isomerization is pH independent, are discussed in terms of a possible I_d mechanism. Attempts to further characterize the isomers of Ga(HDFO)$^+$ by 2D NMR were only partially successful, due to the complexity of the spectra. The results of these combined studies show that Ga is a good substitute metal for Fe in the M-DFO system. Further, it shows that there are only two significant isomers in solution for the labile Ga(III) complex, and these are most likely the N-cis,cis and C-trans,trans isomers.

Introduction

One of the tangential results of research on the siderophores[2] has been the development of clinical iron sequestering agents modeled after, or actually composed of, the natural products.[3] Desferrioxamine B (DFO) is a siderophore produced by *Strep-*

* Author to whom correspondence should be addressed.

(1) Coordination Chemistry of Microbial Iron Transport. 41. For the previous paper, see: Cass, M. E.; Garrett, T. M.; Raymond, K. N. *J. Am. Chem. Soc.* **1989**, *111*, 1677.

0020-1669/89/1328-3538$01.50/0

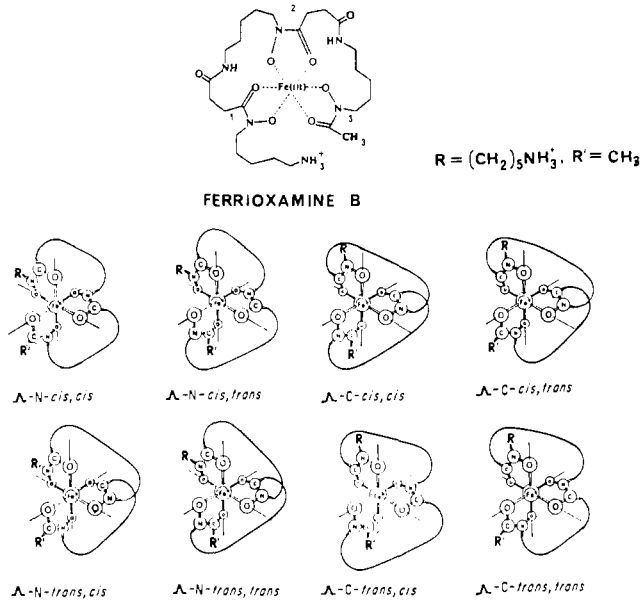

Figure 1. Structure of ferrioxamine B. The drawing at the top of the figure shows the complex in the prevalent protonated state (pH 2–10). Below are shown the eight geometric isomers of the complex. Each is drawn (arbitrarily) as the Λ isomer configuration.

tomyces pilosus, which has become important because of its current use in the treatment of individuals with either acute[4] or chronic iron poisoning.[5] Given as a slow, continuous infusion, it is the current drug of choice for iron chelation therapy of individuals receiving regular blood transfusions for the treatment of Cooley's anemia (β-thalassemia).[6] Desferrioxamine B has also been investigated for use with ^{67}Ga as a contrast agent for radiography.[7]

Desferrioxamine B is a linear trihydroxamic acid composed of alternating 1,5-diaminopentane and succinic acid residues. As the free ligand (H_4DFO^+), it has four acidic protons (three hydroxamic acid groups and one terminal amine); it is positively charged and is readily soluble in water and alcohols. In the presence of ferric ion it forms a cationic, six-coordinate complex (ferrioxamine B, Figure 1) that is thermodynamically stable from pH 2 to pH 10.[8] Theoretically, the ligand can wrap around the metal in 16 ways, resulting in eight distinct geometrical isomers (plus their enantiomeric mirror images). These isomers are depicted schematically in Figure 1. The nomenclature system has been described previously.[9] The DFO ligand itself is achiral; hence, the Δ and Λ isomer sets are true mirror images of each other and are chemically indistinguishable, and these designations will be dropped in the following discussion.

Previous studies of the kinetically inert Cr(III)-substituted complex showed that three fractions were separable by ion-exchange chromatography[10] (only two bands were observed in the first study).[9] On the basis of their retention times and UV–vis spectra, the second and third fractions were assigned as the C-cis,cis and the N-cis,cis isomers, respectively. The first fraction isolated was assumed to be composed of a possible mixture of the six remaining trans isomers; which isomers were actually present could not be determined. From a consideration of CPK molecular models, the N-trans,trans, C-cis,trans, and C-cis,cis isomers are expected to have higher strain energies, since they require the ligand to span trans sites on the coordination octahedron, resulting in very limited flexibility.

In an effort to characterize the thermodynamically stable isomers of $M(HDFO)^+$, studies on the Al(III) and Ga(III) complexes in solution were undertaken. These ions were chosen because they are diamagnetic, allowing the NMR spectra of the metal-bound ligand to be observed. By virtue of its size and the absence of ligand field effects, Ga(III) is expected to behave kinetically and thermodynamically like the native ferric ion; it has often been used as an iron substitute for NMR studies on siderophores.[2,11] However, in enterobactin-mediated iron transport gallium behaves very differently from Fe^{3+}.[12] Therefore, detailed solution studies of the $Ga(HDFO)^+$ complex assessing the actual similarity of Ga(III) and Fe(III) were undertaken to augment the previous structural comparison of relevant Ga(III) and Fe(III) complexes.[13]

Experimental Section

Physical Measurements. UV–vis absorbance measurements were made on either HP8450A or Cary 118 spectrophotometers. IR spectra were recorded on a Perkin-Elmer 283 grating spectrometer. Ion-exchange chromatography was aided by a Gilson 202 fraction collector with the column flow rate controlled by a Buchler polystaltic pump. The eluent was monitored continuously by a Pharmacia UV-2 dual-path monitor.

Potentiometric titrations were performed on a locally built automatic titrator composed of a Metrohm 655 Dosimat titrator and a Fischer Accumet Model 825MP digital pH meter equipped with a Sigma combination glass electrode calibrated with standard acid and base solutions to read hydrogen ion concentration as $-\log [H^+]$. The titration system was controlled by a Commodore 64 computer with locally written software.

NMR measurements were performed on three high-field spectrometers: two custom-built instruments equipped with 4.7-T (UCB-200) and 5.9-T (UCB-250) cryomagnets and controlled by Nicolet NTCFT software, and a commercial Bruker AM-500 spectrometer (11.7-T magnet) controlled by a Bruker Aspect 3000 data system. Correlation spectroscopy (2D) experiments were done on the AM-500 instrument. Variable-temperature ^{13}C measurements were performed on the UCB-200 instrument, using a temperature controller stable to within ±0.5 °C.

Synthesis. Materials. Desferrioxamine B was supplied as a generous gift from CIBA-Geigy Corporation as Desferal, the mesylate salt of the ligand, and was used as received. $Al(NO_3)_3 \cdot 9H_2O$ was reagent grade from Baker & Adamson. Gallium ingots (99.99%) were from Alfa and were dissolved in HCl to make standardized solutions ~0.1 M in $[Ga^{3+}]$ and $[H^+]$. All other chemicals were reagent grade and used as received.

$[M(HDFO)]CH_3SO_3 \cdot 2H_2O$ (M = Al, Ga). The Al(III) and Ga(III) complexes can be readily obtained in a pure state by adding to the ligand an excess of the metal in the form $M(OH)_3 \cdot xH_2O$. The metal hydroxides were prepared fresh by hydrolysis of 10% excess of the metal with a pH 10 NH_4^+/NH_3 buffer solution or a 0.5 M KOH solution. The resulting gel was centrifuged and washed repeatedly with distilled H_2O. In the preparation of the $Al(HDFO)^+$ complex (the processing for Ga(III) is identical), 0.5 g (0.76 mmol) of ligand was added to a slurry of $Al(OH)_3$ gel in 10 mL of H_2O. The mixture was stirred overnight and filtered and the solvent removed under vacuum to yield 0.43 g (78%). The samples had clean NMR spectra and were pure according to elemental analysis. Anal. Calcd (found) for $AlC_{26}H_{53}N_6O_{13}S$: C, 43.94 (43.26); H, 7.51 (7.49); N, 11.82 (11.79); S, 4.51 (4.66). The IR spectra of the Ga(III) and Al(III) complexes were comparable to those of the ferric and chromic analogues.

Attempts to prepare the complexes according to the procedures previously described for the Fe(III) and Cr(III) complexes[9,11,14] were uniformly unsuccessful. These procedures can result in incomplete exchange

(2) Matzanke, B. F.; Müller-Matzanke, G.; Raymond, K. N. In *Physical and Bioinorganic Chemistry*; Loehr, T. M., Gray, H. B., Lever, A. B. P., Eds., VCH Publishers, Inc.: Deerfield Beach, FL, 1989; pp 1–121.
(3) Raymond, K. N. In *Environmental Inorganic Chemistry*; Irgolic, K. J., Martell, A. E., Eds.; Proceedings, U.S.-Italy International Workshop on Environmental Inorganic Chemistry; VCH Publishers, Inc.: Deerfield Beach, FL, *1985*; p 331.
(4) Ackrill, P.; Ralston, A. J.; Day, J. P.; Hooge, K. C. *Lancet* **1980**, *2*, 692.
(5) Barry, M.; Flynn, D. M.; Letsky, E. A.; Risdon, R. A. *Br. Med. J.* **1974**, *2*, 16.
(6) Weatherall, D. J.; Pippard, M. J.; Callender, S. T. *N. Engl. J. Med.* **1983**, *308*, 456.
(7) (a) Hoffer, P. E.; Samuel, A.; Bushberg, J. T.; Thakur, M. *Radiology* **1979**, *131*, 775. (b) Hammersley, P. A. G. *Eur. J. Nucl. Med.* **1984**, *9*, 467.
(8) Schwarzenbach, G.; Schwarzenbach, K. *Helv. Chim. Acta* **1963**, *46*, 1390.
(9) Leong, J.; Raymond, K. N. *J. Am. Chem. Soc.* **1975**, *97*, 293.
(10) Müller, G.; Raymond, K. N. *J. Bacteriol.* **1984**, *160*, 304.
(11) Jalal, M. A. F.; Galles, J. L.; van der Helm, D. *J. Org. Chem.* **1985**, *50*, 5642.
(12) Ecker, D. J.; Matzanke, B.; Raymond, K. N. *J. Bacteriol.* **1986**, *167*, 666.
(13) Borgias, B. A.; Barclay, S. J.; Raymond, K. N. *J. Coord. Chem.* **1986**, *15*, 109.
(14) Monzyk, B.; Crumbliss, A. L. *J. Am. Chem. Soc.* **1982**, *104*, 4921.

Table I. Solution Thermodynamics of $Ga(HDFO)^+$ (1 M KCl, 25 °C)

reacn	log K	log $K(I = 0)$[a] this work	ref 8
Ligand[b]			
$DFO^{3-} + H^+ = HDFO^{2-}$	10.89 (2)	10.01	...
$HDFO^{2-} + H^+ = H_2DFO^-$	9.609 (6)	8.99	9.25
$H_2DFO^- + H^+ = H_3DFO^0$	9.049 (7)	8.73	8.81
$H_3DFO^0 + H^+ = H_4DFO^+$	8.51 (1)	8.51	8.39
$HDFO^{2-} + 3H^+ = H_4DFO^+$	27.17	26.23	26.45
Metal/Complex[c]			
$Ga^{3+} + HDFO^{2-} = Ga(HDFO)^+$	27.56 (2)		
$Ga(HDFO)^+ + H^+ = Ga(H_2DFO)^{2+}$	1.10 (2)[d]		
$Ga(H_2DFO)^{2+} + H^+ = Ga(H_3DFO)^{3+}$	0.78 (2)[d]		
$Ga(DFO)^0 + H^+ = Ga(HDFO)^+$	10.14 (2)		
$Ga(OH)_4^- + 4H^+ = Ga^{3+} + 4H_2O$	17.57 (5)		

[a] Constants corrected to zero ionic strength according to the equation $K = ([HA]/[HA][A])(\gamma_{HA}/\gamma_H\gamma_A)$; $\log K = \log K_0 + \log \gamma_{HA} - \log \gamma_H - \log \gamma_A$, where $\gamma_i = -A/\sqrt{I}/(1 + \sqrt{I}) + 0.1Iz^2$ and $A = 0.505$ at 20 °C and 0.509 at 25 °C.[34] [b] Values obtained from potentiometric titration by using the program PKAS. [c] Refined by using the program BEST. [d] Obtained from analysis of spectrophotometric titration.

of the counterions or contamination by solvent (ethyl acetate) used in the workup.[14] The method described here is simpler and cleaner: there are no extraneous counterions, and the unreacted starting material, $M(OH)_3$, is readily separated from the highly soluble product.

Chromatography. The Ga and Al complexes of HDFO were chromatographed on AG 50W-X4 (400 mesh) cation-exchange resin as described previously.[9,10] A 1 × 18 cm column was used, and flow rates (typically) were 1 mL/min. The Al and Ga complexes eluted as single bands with elution volumes comparable to that of the trans isomer(s) of $Cr(HDFO)^+$.[10] The eluent was frozen immediately in a dry ice/acetone bath and the solvent removed under vacuum. The NMR spectra recorded at 5 °C for both the leading and trailing edges of the band collected for the $Al(HDFO)^+$ chromatography were identical with each other as well as that for the unchromatographed material. This indicates that isomerization occurs much more rapidly than the time scale of the chromatography experiment. The alternative, that only one isomer is present, is ruled out by the NMR results (see below).

Solution Thermodynamics of $Ga(HDFO)^+$. Potentiometric Titrations. Titrations were performed by using the automatic titrator. Stock KOH was prepared from Baker Dilut-it standards, and standardized against potassium acid phthalate. The solution was stored under oxygen- and carbonate-scrubbed argon (bubbled through a basic pyrogallol solution and passed through Ascarite). Stock HCl was standardized against the KOH. The titrations were performed in water-jacketed vessels maintained at 25 °C. Samples were typically 50 mL and had $[Ga^{3+}]$ and [DFO] concentrations of 0.5 mM. The samples were maintained under argon throughout the titration. Potentiometric titrations were analyzed by using the iterative programs PKAS,[15] for calculating ligand pK_a's and BEST[16] for refining stability constants.

Spectrophotometric Titrations. Desferal was titrated in 1 M KCl while observing the UV spectrum between 200–250 nm. Aliquots of the sample were withdrawn following additions of KOH for absorbance measurements and then returned. The protonation of $Ga(HDFO)^+$ was observed by preparing separate samples at various pH values or by removing aliquots from a bulk solution as it was titrated with acid. Samples were generally about 0.5 mM in $[Ga^{3+}]_0$ and/or $[DFO]_0$.

Results

Thermodynamic Results. Protonation Constants of H_4DFO^+. Refinement of the potentiometric titration data of DFO gives constants for the protonation of each hydroxamate and the terminal amine. These ligand protonation constants are presented in Table I. Allowing for the change in temperature and ionic strength, they are in excellent agreement with the literature values.[8]

Protonation Constants of $Ga(HDFO)^+$. The spectrophotometric titration of $Ga(HDFO)^+$, shown in Figure 2, reveals the gradual development of a shoulder at ~225 nm as the pH is raised from 0.7 to ~2. There is an isosbestic point at 209 nm during this change which corresponds to the formation of the fully complexed

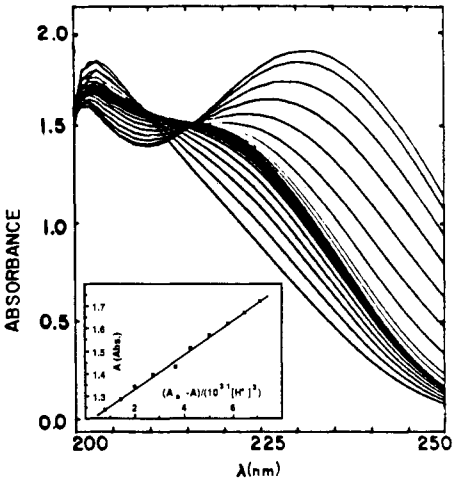

Figure 2. Spectrophotometric titration of $Ga(HDFO)^+$ in 1 M KCl at 25 °C, pH 0.74–11.11, $[Ga]_0 = 1.002$ mM, $[DFO]_0 = 1.022$ mM, 1 mm path length. Inset: Schwarzenbach plot of high pH data from the spectrophotometric titration of $Ga(HDFO)^+$ from pH 10.34 to pH 10.83. The plot is calculated for the reaction $Ga(OH)_4^- + HDFO^{2-} + 3H^+ = 4H_2O + Ga(DFO)$. Absorbances are adjusted for dilution. The slope of this plot gives an apparent constant $\log K \approx 32$. Since there are several equilibrium reactions of significance at this pH (see text), this number is a composite of equilibrium reactions.

$Ga(HDFO)^+$ at pH 2. However, these data did not give a linear Schwarzenbach plot.[8] Numerous titrations resulted in a wide range of values for the protonation constant of the complex, averaging $pK^H \simeq 0.7$ (5). It seems that there is significant decomposition of the siderophore under the acidic conditions of the titration. The absorbance of samples prepared at pH ≤ 1 decreased gradually with time, and raising the pH did not result in the expected increase in absorbance due to metal binding. Similar observations were reported by the Schwarzenbachs for the Fe(III) complex.[8] Numerical analysis of the titration data shown in Figure 2 resulted in two closely spaced protonation constants: $pK_1 = 1.10$ (2) and $pK_2 = 0.78$ (2). Because of the decomposition problem, these values are relatively uncertain. However, they are in general accord with the single protonation constant ($pK^H = 0.94$)[8] observed for $Fe(HDFO)^+$.

From about pH 2 to pH 9 the spectra change very little, indicating that the $Ga(HDFO)^+$ complex is the dominant species in solution. The increase in absorbance at 235 nm that is observed as the pH is brought above 9 is not observed in the ferric complex. However, the spectrophotometric titration of the free ligand shows the same absorption curve at higher pH. This leads to the conclusion that the band at 235 nm arises from unbound deprotonated hydroxamate chromophores. At higher pH the complex is hydrolyzed completely, yielding $Ga(OH)_4$ and anions of DFO. Analysis of the spectral changes at high pH according to the Schwarzenbach method is successful for a three-proton equilibrium. This is shown in Figure 2 (inset).

The principal equilibrium reactions (and their associated equilibrium constants) at high pH are

$$Ga(OH)_4^- + HDFO^{2-} + 3H^+ = 4H_2O + Ga(DFO)^0 \quad \log K = 34.99 \quad (1)$$

$$Ga(DFO)^0 + H^+ = Ga(HDFO)^+ \quad \log K = 10.14 \quad (2)$$

$$HDFO^{2-} + H^+ = H_2DFO^- \quad \log K = 9.61 \quad (3)$$

For total metal complex concentrations of about mM (this study) this means that all three of the above reactions are significant between pH 9.6 and 10.1, with the equilibrium shifting to the left side as the pH is raised.

Stability Constant for $Ga(HDFO)^+$. The very large equilibrium constants of powerful chelating agents such as DFO lead to practically complete complexation of the metal. Since reaction 4 lies almost entirely to the right near neutral pH, estimation of

$$M^{3+} + H_4DFO^+ \rightleftarrows M(HDFO)^+ + 3H^+ \quad (4)$$

(15) Motekaitis, R. J.; Martell, A. E. *Can. J. Chem.* **1982**, *60*, 168.
(16) Motekaitis, R. J.; Martell, A. E. *Can. J. Chem.* **1982**, *60*, 2403.
(17) Davies, C. W. *J. Chem. Soc.* **1938**, 2093.

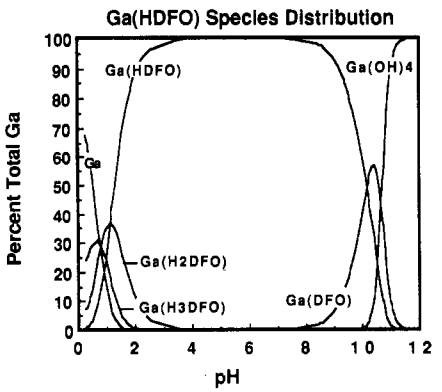

Figure 3. Species distribution plot for the $Ga(HDFO)^+$ system, pH 0–12, $[Ga]_T$ = 1 μM, $[DFO]_T$ = 10 μM. The plot is based on equilibrium constants reported in Table I. Only metal-containing species with greater than 1% abundance are shown.

the free metal ion concentration by the difference of $[M]_{total} - [M]_{bound}$ is not reliable. Unlike the ferric ion, the equilibria of Ga^{3+} that involve hydroxide species are rapid. A significant difference is also found in the relative stabilities of the $M(OH)_4^-$ species of Fe and Ga. Both $M(OH)_3$ species have similar hydrolysis constants for the reaction leading to the trihydroxide:

$$M^{3+} + 3H_2O = M(OH)_3(aq) + 3H^+ \quad K_{13} \qquad (5)$$

The values of log K_{13} are −11.63 for Ga and ≤−12 for Fe.[18] For the reaction

$$M^{3+} + 4H_2O = M(OH)_4^- + 4H^+ \quad K_{14} \qquad (6)$$

log K_{14} for gallium is 4 orders of magnitude larger than the iron constant, −17.5 versus −21.6 (adjusted to 1 M ionic strength).[18] Consequently the competition between DFO and OH^- for Ga^{3+} binding can be used to measure the stability of the Ga(DFO) complex.

Refinement of the β's (overall formation constants) for $Ga(OH)_4^-$, $Ga(HDFO)^+$, and Ga(DFO) against potentiometric titration data with the program BEST[16] gave the thermodynamic results presented in Table I. The good agreement between the hydrolysis constant for $Ga(OH)_4^-$ refined here and that reported in the literature[18] is a gauge of the reliability of both the data and the model used in this refinement. The overall results are in agreement with general expectations; gallium complexes tend to be less stable by a few orders of magnitude than the analogous iron complexes.[13]

A plot of the species distribution as a function of pH is shown in Figure 3; the only significant species from pH 2–9 is the fully coordinated, cationic species $Ga(HDFO)^+$. From a thermodynamic perspective, the Ga and Fe complexes are essentially interchangeable over a very broad range of pH.

NMR Results. NMR Spectroscopy of H_4DFO^+. The proton spectrum of Desferal in DMSO-d_6 recorded at 250 MHz and 21.5 °C is very simple, revealing considerable pseudosymmetry for this trihydroxamic acid (Figure 4). Note, however, that the three hydroxamic acid protons are resolved (inset) at 9.70–9.64 ppm. The amide and amine protons are at 7.85 and 7.70 ppm, respectively. The hydroxamate and amine protons exchange immediately with added D_2O while the amide protons exchange more slowly. The full assignment of the proton and carbon NMR spectra was achieved by means of homonuclear and heteronuclear correlation spectroscopy at 500 MHz, in D_2O. The results are given in Table II. A phase-sensitive, double-quantum-filtered COSY[20,21] spectrum (Figure 5, supplementary material[22]) was used to distinguish the protons of the N-terminal diaminopentyl chain.

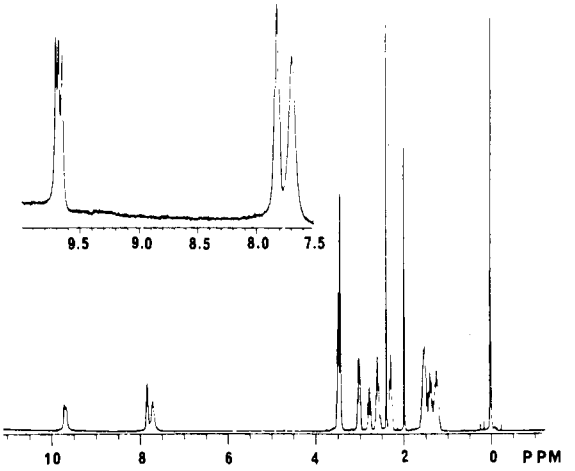

Figure 4. ^1H NMR spectrum of $H_4DFO{\cdot}CH_3SO_3$ (Desferal) in DMSO-d_6, at 250 MHz and 21.5 °C.

Table II. ^1H and ^{13}C NMR Chemical Shifts (ppm) of $H_4DFO{\cdot}CH_3SO_3$ (Desferal)

	^1H		^{13}C
	DMSO-d_6 (250 MHz)	D_2O (500.1 MHz)	D_2O (125.7 MHz)
CH_3	1.98	2.14	20.11
C=O			174.34
N—OH	(9.64, 9.67, 9.70)		
CH_2	3.46	3.62 (^3J = 6.9 Hz)	48.53, 48.70
CH_2	1.50	1.63	26.30
CH_2	1.21	1.31	23.91
CH_2	1.37	1.52	28.75
CH_2	3.00	3.17 (^3J = 6.75 Hz)	40.01
NH	7.85		
C=O			175.55
CH_2	2.29	2.50 (^3J = 6.95 Hz)	31.18, 31.31
CH_2	2.59	2.80 (^3J = 6.95 Hz)	28.43, 28.49
C=O			174.61, 174.75
N—OH	(9.64, 9.67, 9.70)		
CH_2	3.46	3.64 (^3J = 6.8 Hz)	48.47
CH_2	1.50	1.67	26.11
CH_2	1.21	1.37	23.49
CH_2	1.37	1.70	27.12
CH_2	2.79	3.00 (^3J = 7.6 Hz)	40.17
NH_3^+	7.70		
$CH_3SO_3^-$	2.39	2.81	39.31

Once the protons were identified, the high-field part of the carbon spectrum (aliphatic) was easily assigned by means of a proton–carbon correlation spectrum (Figure 6, supplementary material[22]). The protonation dependence of the carbonyl region was used to identify the hydroxamate peaks: as the molecule is deprotonated, the three peaks between 174.3 and 174.8 ppm shift upfield, as expected from the increased electron density on the carbon (Figure 7). Another experiment confirmed this result: two spectra of the carbonyl region were acquired with selective proton decoupling at either 2.80 or 2.50 ppm (i.e. the succinyl

(18) Baes, C. F., Jr.; Mesmer, R. E. *The Hydrolysis of Cations*; John Wiley and Sons: New York, 1976; pp 226–237, 313–319.
(19) Martell, A. E.; Smith, R. M. *Critical Stability Constants*; Plenum: New York, 1977.
(20) Marion, D.; Wüthrich, K. *Biochem. Biophys. Res. Commun.* **1983**, *113*, 967.
(21) Rance, M.; Sorensen, O. W.; Bodenhausen, G.; Wagner, G.; Ernst, R. R.; Wüthrich, K. *Biochem. Biophys. Res. Commun.* **1983**, *117*, 479.

(22) See note regarding supplementary material at end of this paper.

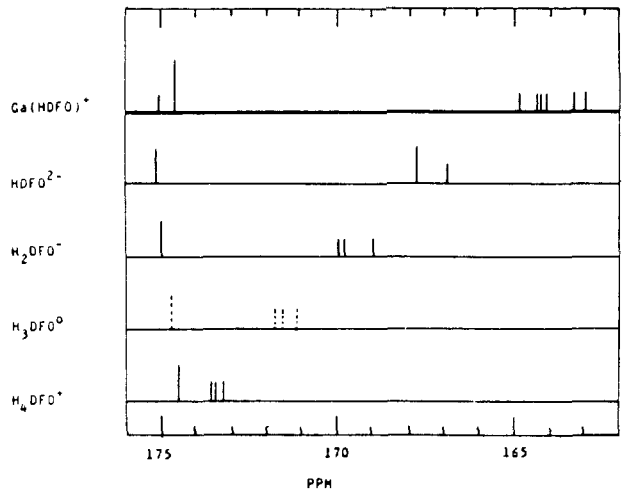

Figure 7. Schematic representation of the effect of deprotonation and metal complexation on ^{13}C spectrum of Desferal (carbonyl region only). The dashed line spectrum for H_3DFO^0 is not experimentally observed. It is drawn to aid in visualizing the shifts accompanying the deprotonation of the ligand.

protons). The importance of the nuclear Overhauser effect (NOE) on neighboring carbons depends on their distance from the irradiated protons. Thus decoupling at 2.80 ppm will preferentially enhance the hydroxamate carbonyl peaks, and irradiation at 2.50 ppm will instead enhance the amide carbonyl peaks. Figure 8 shows both spectra and the difference spectrum obtained by their subtraction, which assigns unambiguously the peak at 175.55 ppm to the amides and the peaks at 174.71 and 174.65 ppm to the hydroxamates. Moreover, the peak at 174.34 ppm, which is not enhanced in either spectrum, can be attributed to the C-terminal hydroxamate carbonyl; the smaller deshielding effect of CH_3 vs CH_2 might explain its slightly upfield position. This experiment also provides an indirect confirmation of the proton assignment in the succinyl moieties.

Several desferrioxamines (A_1, B, D_1, E, G and H) have been studied[23] by ^1H and ^{13}C NMR spectroscopy at 100 and 300 MHz and 24 and 75 MHz, respectively and their spectra were assigned by comparison between these closely related molecules and occasionally by using spectra from derived products or synthetic model compounds. Our results for desferrioxamine B are in very good agreement with those, except for a few assignments in the ^{13}C spectra that required 2D correlation spectroscopy.

NMR Spectroscopy of M(HDFO)$^+$. In contrast with the apparent simplicity of the ligand spectra, the ^{13}C (and particularly ^1H spectra) of the metal complexes contain many more features. Preliminary examination of the ^{13}C spectra revealed that there were six lines in the hydroxamate carbonyl region, six lines for the CH_2 groups attached to them, and four lines for the CH_2 groups α to the amide nitrogens (Figure 9). This suggests the presence in solution of essentially *two* isomers in similar proportions. Since there appears to be no significant different between the Al(III) and Ga(III) complexes, the in-depth analysis of the NMR features will be limited to the latter, which is the better model for ferrioxamine.

The two isomers interconvert at a rate on the order of magnitude of the NMR time scale. In order to slow down the isomerization, and thus minimize exchange broadening of the peaks, the spectra intended to identify the resonances of each isomer were recorded between 7 and 10 °C. The same 2D correlation experiments used for the ligand alone were repeated for the gallium complex. However, the presence of the metal center makes the molecule chiral, and most of the CH_2 groups consist of diastereotopic protons; thus, to nearly each of the methylene peaks in the ligand proton spectrum correspond *four* peaks in the gallium complex spectrum, with intensities reduced accordingly. As a consequence, resulting spectra are much harder to interpret (Figure 10, supplementary material[22]). In some instances, it was impossible to identify cross-peaks where they should have appeared on the 2-D map because of the overlap of neighboring features. The succinyl protons exemplify this: between 2.4 and 2.8 ppm (this is 200 Hz),

(23) Huber, P. Ph.D. Thesis, Diss. ETH Nr. 7077, Zürich, 1982.

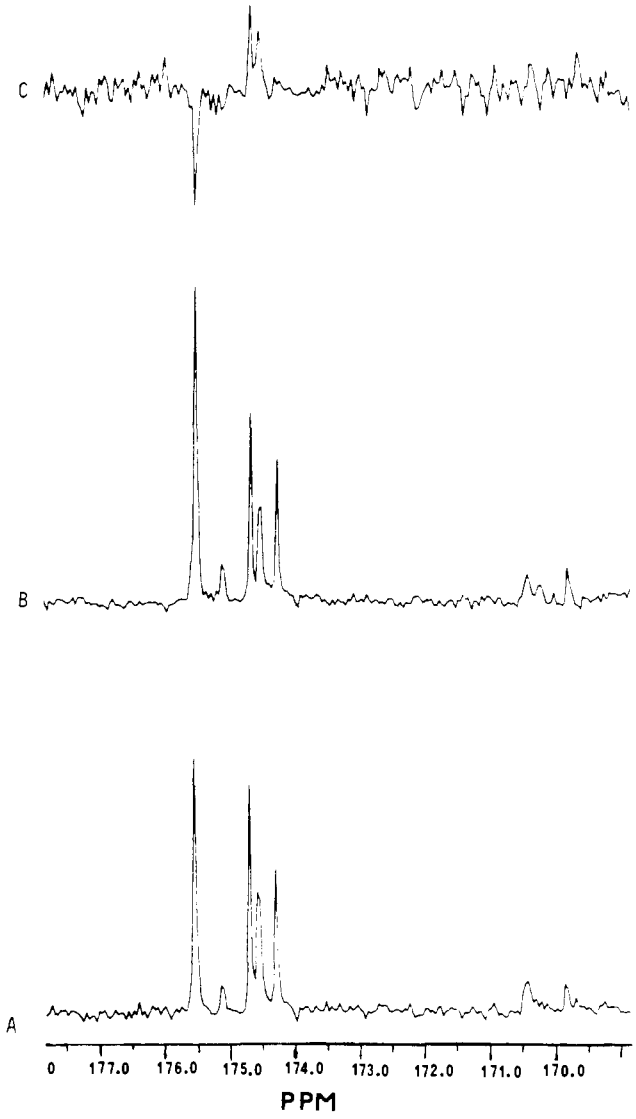

Figure 8. Heteronuclear difference NOE experiment on 0.16 M H_4DFO^+ in D_2O, at 500 MHz and 22 °C. ^{13}C spectra were recorded with 1840 transients of 512 data points over 1292 Hz (10.3 ppm), in the carbonyl region. Spectra A and B were obtained with selective ^1H irradiations at 2.80 and 2.50 ppm, respectively. The difference between A and B gives spectrum C.

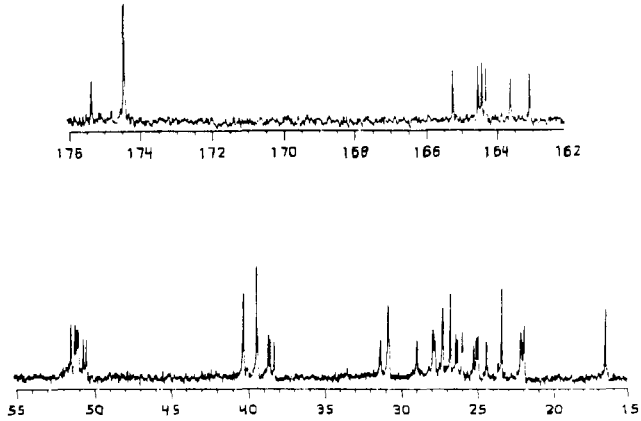

Figure 9. ^{13}C NMR spectrum of Al(HDFO)$^+$ in D_2O. Note the six-line patterns for the hydroxamate carbonyls (165.6–163 ppm) and $N(O)CH_2$ (52–50 ppm) groups and the four-line pattern for the amide NCH_2 (39.5–38 ppm) groups, which are evidence of two isomers.

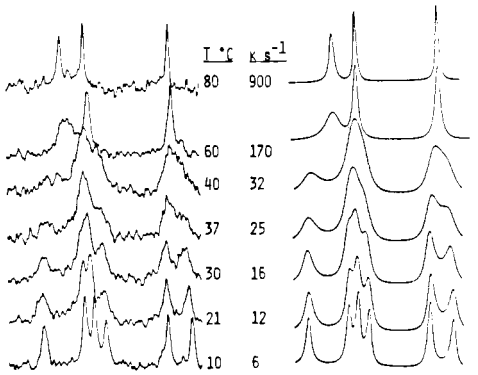

Figure 11. Temperature-dependent ^{13}C NMR spectra of Ga(HDFO)$^+$ in D_2O. The FID's were multiplied by an exponential function prior to Fourier transformation to improve signal/noise ($A = A_0e^{-n(2\pi/SW)}$; where n is the number of the data points being multiplied, and SW is the spectral window in Hz). Calculated spectra in the right hand of the figure are generated by the program DNMR3 (see ref 24 and 25). Input to the program included the low-temperature (slow-exchange) chemical shifts of the exchanging nuclei, a rate constant, an isomerization scheme that interconverts peaks 1 ↔ 3, 2 ↔ 4, and 5 ↔ 6 (peak 1 is at lowest field, peak 6 at highest), and the effective relaxation rate $1/T_2^*$ as determined from the line width of nonexchanging peak ($-CH_3$). This incorporates the additional line broadening due to the exponential multiplier.

four strongly coupled AA'BB' systems are intertwined. In most cases, however, it was possible to assign the proton and carbon resonances. The next challenge was, by use of the COSY spectrum, to link these individual pieces into chains belonging to one or the other isomer. As shown in Table III, this was only partially achieved. The CO–NO and CO–NH moieties are effective barriers to magnetic coupling, so the diaminopentyl and succinyl residues cannot be connected. Moreover, the γ methylenes of the "inner" diaminopentyl chains all have approximately the same ^1H chemical shifts, presumably because they are so far from the coordination site. Therefore the cross-peak "tracks" on the COSY map converge to the same point, and the complete diaminopentyl chains cannot be distinguished and uniquely assigned.

Finally, to assign peaks for interconverting groups, a ^{13}C spectrum was obtained at 80 °C, and the chemical shifts of the coalesced peaks were compared to those in the low-temperature spectrum. In most cases, the average chemical shift between two interconverting peaks was less than 0.2 ppm away from the coalesced peak chemical shift, which removed any ambiguity.

Temperature Dependence of Isomerization in Ga(HDFO)$^+$ Solutions. ^{13}C spectra of a 0.15 M Ga(HDFO)$^+$ sample in D_2O (uncorrected pD 6.8) were recorded at 50 MHz between 10 and 80 °C. The probe temperature was allowed to equilibrate for ~10 min prior to final magnetic field homogeneity optimization on the ^1H FID. Spectra consisted of 10000 transients collected with a 1.47-s recycle time. Internal p-dioxane (δ 67.4 ppm) was used as a chemical shift reference. The experimental spectra of the hydroxamate carbonyl region were simulated by using Binsch and Kleier's DNMR3 program[24] as modified by Bushweller.[25] The rate constants are calculated for conversion of the most abundant isomer (represented by peaks 2, 3, and 5) to the other isomer (represented by peaks 1, 4, and 6). The results are shown in Figure 11.

A test of the pD dependence of the isomerization was made by recording spectra of samples with pD 2.5, 4.3, and 10.1 at 35 °C (near the coalescence temperature for the pD 6.8 sample). No difference was observed in the spectra. The kinetics of isomerization were also followed in methanol-d_4 and DMSO-d_6. These spectra are presented in Figure 12. The rate constants for isomerization in these solvents were determined by matching the line shapes of just the two peaks furthest upfield by using the Nicolet NTCXCH program.[26] In the case of DMSO-d_6, coalescence had already occurred at 21 °C, the lowest temperature for which spectra could be recorded in this solvent (mp 18 °C). This is in contrast to the higher coalescence temperatures in D_2O and methanol-d_4. In order to estimate the rate constants for the DMSO spectra, the chemical shift difference between the peaks giving rise to the observed spectrum was assumed to be the same as in the Al(HDFO)$^+$ complex. This assumption certainly leads to small systematic errors, but it was desired to obtain at least a crude measure of the isomerization rate in DMSO.

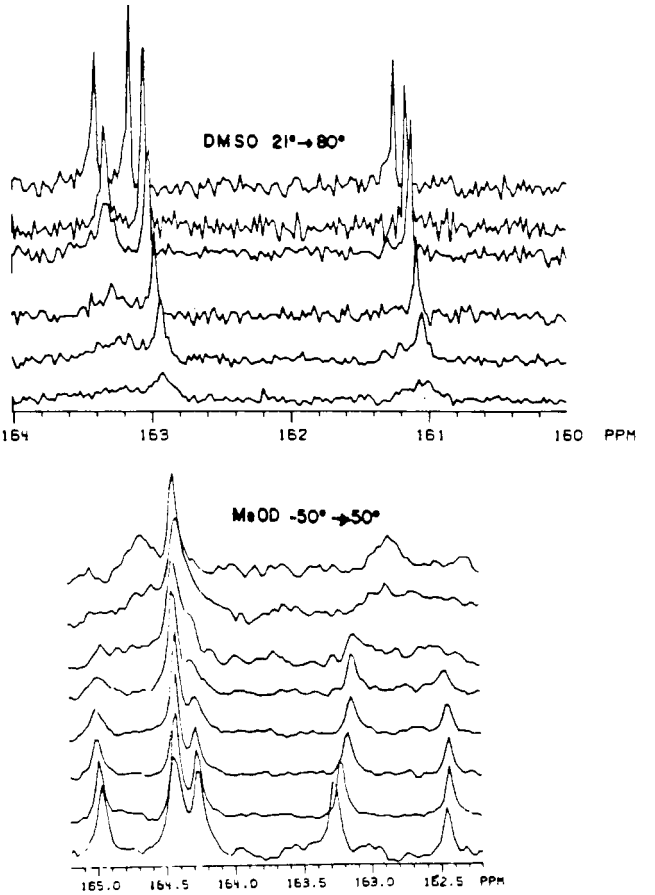

Figure 12. Temperature-variable ^{13}C NMR spectra of Ga(HDFO)$^+$ in methanol-d_4 (−50, −30, −10, +1, +11, +21.5, +36, and +50 °C from bottom to top) and DMSO-d_6 (+21, +30, +40, +50, +60, and +80 °C from bottom to top).

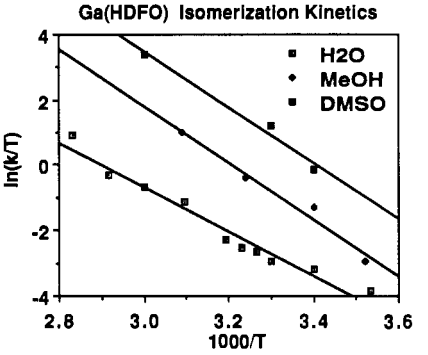

Figure 13. Plot of the kinetic data for isomerization of Ga(HDFO)$^+$ in D_2O, methanol-d_4, and DMSO-d_6. Rate constants are plotted as ln (k/T) versus $1/T$. The slopes of the lines are equal to $\Delta H^*/R$. ΔS^* values are calculated from the intercepts. Only the spectra ≥10 °C were analyzed for the methanol-d_4 data since the rate of exchange was too slow to be accurately determined from the lower temperature spectra. Only three spectra were analyzed for the DMSO data since only a qualitative measure of the kinetics could be obtained (see text).

(24) Kleier, D. A.; Binsch, G. Quantum Chemistry Program Exchange No. 165.
(25) Bushweller, C. A.; Bhat, G.; Lelandre, L. J.; Brunelle, T. A.; Bilofsky, H. S.; Ruben, H.; Templeton, D. A.; Zalkin, A. *J. Am. Chem. Soc.* **1975**, *97*, 65.
(26) Users' guide for the Nicolet NTCXCH program. UCB NMR facility.

Table III. ^1H and ^{13}C NMR Chemical Shifts (ppm) of $Ga(HDFO)^+$, in D_2O at 9 °C[a]

CH_3	2.191 [17.19] ↔ 2.203 [17.12]
CO	[162.91] ↔ [163.38]
NO	
CH_2	{3.545/3.956 [51.08]} ↔ {3.576/3.984 [50.73]} {3.560/3.970 [51.78]} ↔ {3.591/4.107 [51.39]}
CH_2	{1.551/1.891 [26.48]} ↔ {1.480/1.808 [25.98]} {1.465/1.850 [26.10]} ↔ {1.510/1.819 [26.34]}
CH_2	1.21–1.22 [21.94; 22.17]
CH_2	{1.440/1.660 [29.13]} ↔ {1.497 [27.88] / 2.925/3.479 [38.90]} {1.476 [27.99] / 2.898/3.469 [38.74]} ↔ {1.556 [27.99] / 2.951/3.492 [38.56]}
CH_2	{3.156/3.316 [39.38]}
NH	
CO	174.58; 174.64 ↔ 175.46
CH_2	{2.604/2.789 [30.93]} ↔ {2.604/2.789 [30.93]} {2.535/2.807 [30.81]} ↔ {2.577/2.775 [31.21]}
CH_2	{2.444/2.979 [25.00]} ↔ {?/? [25.59]} {?/3.113 [25.51]} ↔ {?/3.071 [25.74]}
CO	
NO	$_2$
CH_2	{3.73/3.84 [51.49]} ↔ {3.67/3.89 [51.67]}
CH_2	{1.796 [26.80]} ↔ {1.801 [26.80]}
CH_2	1.410 [23.41]
CH_2	1.729 [27.28]
CH_2	3.022 [40.13]
NH_3^+	

[a] The ^{13}C shifts are between square brackets; frequencies of diasterotropic protons are separated by a slash. Large braces join methylene groups that belong to the same isomer; arrows denote interconverting groups.

The calculated rate constants are fitted as a function of $1/T$ according to eq 7. The results are plotted in Figure 13, and the

$$\ln\left(\frac{k}{T}\right) = -\frac{\Delta H^\ddagger}{R}\left(\frac{1}{T}\right) + \frac{\Delta S^\ddagger}{R} + \ln\left(\frac{R}{Nh}\right) \qquad (7)$$

kinetic parameters ($\Delta H^\ddagger$, $\Delta S^\ddagger$, and k(298 K)) derived from these fits are presented in Table IV.

Discussion of the Isomerization Mechanism. In D_2O the isomerization is essentially proton independent over the range of pH where the complex is stable (pH ~2–10). This rules out mechanisms that require protonation of one of the hydroxamate arms. It was anticipated that the reaction *would* involve a protonation concomitant with dissociation of one ligand arm, which, when recomplexed in a different orientation, would yield isomerization. This apparently is not the case.

The negative activation entropy, $\Delta S^\ddagger = -10$ (3) cal·K^{-1}·mol^{-1}, might seem suggestive of an associative (A or I_a) mode of activation for the isomerization. However, it is dangerous to assign mechanisms on the basis of activation parameters alone. Holm and co-workers[27] have explicitly argued against the use of activation parameters, particularly $\Delta S^\ddagger$, as the sole criterion for establishing mechanism. Indeed, the contributions from solvent restructuring to the entropy of the transition state (rather than changes in the inner coordination sphere) may well be the overriding consideration. Solvent structure changes are the principal cause of the hydrophobic effect as described by Tanford.[28] The same considerations may be operative here. Water is a highly ordered solvent characterized by the formation of many transient hydrogen bonds. When a nonpolar solute is introduced into this environment, the hydrogen-bonding network is disrupted in the vicinity of the solute, and the structure of the water is modified. However, it is not generally true that there will be a net breaking of bonds and loss of structure. Instead, new hydrogen bonds are formed, and there can be a substantial increase in order induced by the formation of an ordered hydration shell around the solute. Ionic solutes can have the opposite effect of inducing a net loss of water structure even though the first coordination sphere of the ion is well ordered.[29] We will follow several lines of deductive reasoning in presenting the possible mechanism for the isomerization.

Monzyk and Crumbliss,[14] in their study on the dissociation kinetics of $Fe(HDFO)^+$, postulate a reaction scheme in which the first step is a proton-independent attack by H_2O leading to a

Table IV. Kinetic Parameters for Isomerization of $Ga(HDFO)^+$ in D_2O, Methanol-d_4, and DMSO-d_6[a]

	solvent		
	D_2O	methanol-d_4	DMSO-d_6
k(298 K)/s^{-1}	13 (1)	73 (7)	4.1 (6) × 10^2
$\Delta H^\ddagger$/kcal·mol^{-1}	13 (1)	17 (2)	17 (5)
$\Delta S^\ddagger$/cal·mol^{-1}·K^{-1}	−10 (3)	+8 (8)	+10 (15)

[a] The standard deviations reported for $\Delta S^\ddagger$ correspond to the difference between the limits predicted by the 1σ slopes.

(27) Hutchison, J. R.; Gordon, J. R., II; Holm, R. H. *Inorg. Chem.* **1971**, *10*, 1004. These authors suggested dissociative mechanisms were unlikely for isomerization of M(1-phenyl-5-methylhexane-2,4-dionate)$_3$ in chlorobenzene in spite of positive activation entropies of +13 and +3 cal·K^{-1}·mol^{-1}, respectively for M = Al or Ga. There are numerous examples in which activation entropies of opposite sign nevertheless correspond to similar mechanisms. For example, Co(5-methylhexane-7,4-dionate)$_3$ and Co(benzoylacetonate)$_3$ also both rearrange via a bond rupture mechanism in chlorobenzene and have positive activation entropies (+7 and +10 cal·K^{-1}·mol^{-1}): Gordon, J. G., II; Holm, R. H. *J. Am. Chem. Soc.* **1970**, *92*, 5319. Girgis, A. Y.; Fay, R. C. *J. Am. Chem. Soc.* **1970**, *92*, 7061. On the other hand $Cr(C_2O_4)^{3-}$ and Cr(en)$(C_2O_4)^-$ racemize in water via a bond rupture mechanism, but with negative activation entropies (−24 and −27 cal·K^{-1}·mol^{-1}): Busbra, E.; Johnson, C. H. *J. Chem. Soc.* **1939**, 1937. Conversely, twist mechanisms are found in the racemization in aqueous solution of Fe(phen)$_3^{2+}$ and Co(EDTA)$^-$, which both have large positive activation entropies (+21 cal·K^{-1}·mol^{-1}): Basolo, F.; Hayes, J. C.; Neumann, H. M. *J. Am. Chem. Soc.* **1954**, *76*, 3807. Cooke, D. W.; Im, Y. A.; Busch, D. H. *Inorg. Chem.* **1962**, *1*, 13.

(28) Tanford, C. *The Hydrophobic Effect: The Formation of Micelles and Biological Membranes*; Wiley: New York, 1980; pp 24–27.

(29) Frank, H. S.; Evans, M. W. *J. Chem. Phys.* **1945**, *13*, 507.

seven-coordinate intermediate. This intermediate is subsequently protonated, and the chelate arm (presumed to be the N-terminal hydroxamate) dissociates. The rate of isomerization for Ga(HDFO)$^+$ determined in the present study is comparable to the rate of the initial solvent attack on Fe(HDFO)$^+$, consistent with a similar mechanism. We note, however, that high-pressure NMR results[30] show that solvent exchange on Ga^{3+} proceeds dissociatively, while for Fe^{3+} an associative process is indicated. This difference was attributed to the electronic configuration of the metal ions; electron-poor ions tend toward associative solvent exchange while electron-rich ions undergo dissociative exchange. This result, though strictly relevant only to solvent exchange, gives support to a concerted I_a or perhaps I_d mode of isomerization over a purely associative (A) mechanism. Such a concerted I_a or I_d mechanism, with participation of a molecule of water (possibly promoting interconversion through hydrogen bonding) at the transition state, is consistent with the $\Delta S^\ddagger$ values, since expansion of the coordination sphere and an increase in local ordering of the water structure in the transition state give opposing changes in entropy. We favor the I_d mechanism since it is more consistent with the dissociative mode of solvent exchange at Ga. It is also consistent with the results of isomerization in both MeOH and DMSO. In both solvents, the reaction is *faster* than in H_2O. If the mode of activation was associative (and preserved upon changes in solvent), the reaction should be slower in these bulkier solvents, not faster. As seen in Figure 13 and Table IV, the increase in rate is primarily due to a change in activation entropy (the plots are roughly parallel). Neither MeOH nor DMSO form solvent structure as readily as H_2O; hence, any solvent structure entropy contributions will be minimized in these solvents, and the positive entropy contribution due to the flexibility of the complex will dominate.

We expect solvents with lower dielectric constants (compare $\epsilon(H_2O) = 78.5$, $\epsilon(MeOH) = 32.5$, and $\epsilon(DMSO) = 47.6$)[31] to interact less strongly with charged species. It might seem attractive to assign the solvent-dependent change in activation entropy to the interaction of the positively charged amine "tail" of DFO with the negative hydroxamate groups of the complex. However, there is no other evidence of interaction between the amine and hydroxamate groups. This interaction would be expected to depend on the solvent's dielectric strength. The chemical shift of the methylene carbon adjacent to the terminal amine is essentially constant for free and complexed ligands in D_2O, methanol-d_4, or DMSO-d_6. Thus, there is no apparent change in the hydrogen-bonding character of the amine with respect to metal coordination or solvent changes. Moreover, in the crystal structure of the closely related ferrioxamine D_1[32] (identical with ferrioxamine B except than an acetyl group replaces a proton on the terminal amine, creating a neutral complex), the terminal chain is held somewhat away from the coordination octahedron by a hydrogen bond between the terminal amine and the amide carbonyl of the adjacent succinyl unit. Thus, while there is an intramolecular terminal amine hydrogen bond, it seems to have no influence on the metal coordination center.

Summary

The thermodynamic results of this study show that the Ga complex is very much like the ferric complex, with the exception of the hydrolysis observed at high pH. These results support the expectation that information gained by studying the Ga complex will be transferable to the natural Fe complex.

The NMR study shows that only *two* isomers of Ga(HDFO)$^+$ (and presumably Fe(HDFO)$^+$) have appreciable significance in solution. This is in contrast to the chromic complex, where at least three isomers were observed. The ultimate goal of the 2D experiments at very high field was to identify these isomers. Examination of CPK models of the different isomers shows that some (unconnected) protons are closer in some isomers than in others, and it was hoped that a NOE correlation (NOESY)[33] spectrum would show specific cross-peaks allowing determination of the isomer geometries. However the complexity of the Ga(HDFO)$^+$ spectra precluded this. Arguments regarding the relative stability of these isomers based on their presumed strain energies are at best qualitative. However, we believe that the most likely isomers are the N-cis,cis and C-trans,trans ones. These are interconverted in principle simply by flipping the N-terminal hydroxamate. Their assignment is also supported by the following: (1) of the two cis,cis isomers allowable, the N-cis,cis appears to be less strained; (2) the simplest isomerization process will effectively flip just one hydroxamate; (3) the dissociation kinetics of Monzyk and Crumbliss[14] indicate that the N-terminal hydroxamate is the most labile. Additionally, the chemical shifts of the interconverting hydroxamate carbonyls provide a clue to the isomer identities. Of the pairs of interconverting peaks, 1 ↔ 3 (Figure 11) have the largest splitting, suggesting that the carbonyl assigned to these peaks experiences the greatest change in environment. The splitting between peaks 2 ↔ 4 and 5 ↔ 6 are similar to each other and smaller than the 1 ↔ 3 splitting. Changing just the N-terminal hydroxamate will have the effect of moving the N-terminal carbonyl from a coordination face shared by three carbonyls to a face with two nitroxides and one carbonyl. Similarly, the middle hydroxamate and C-terminal hydroxamates will end up in an environment that is less perturbed: two carbonyls and one nitroxide. This result is consistent with the proposal that the thermodynamically significant isomers in solution for Ga(HDFO)$^+$ are N-cis,cis and C-trans,trans.

The kinetics of isomerization between the two isomers (a) are not catalyzed by H^+, (b) are comparable to the corresponding initial steps of the ligand exchange process, and (c) show enthalpies of activation with relatively small activation barriers. These observations favor an intramolecular rearrangement process that involves neither explicit solvent association nor metal–hydroxamate dissociation in the transition state.

Acknowledgment. We thank Dr. D. J. Meyerhoff for providing the heteronuclear NOE difference experiments and for useful discussions about the 2D NMR spectra. A.D.H. thanks the Stiftung für Stipendien auf dem Gebiete der Chemie for a scholarship. This research was supported by NIH Grant AI 11744.

Supplementary Material Available: Figures 5, 6, and 10, showing a phase-sensitive DQ-COSY spectrum of HDFO$^+$, a ^1H–^{13}C correlated spectrum of HDFO$^+$, and a phase-sensitive DQ-COSY spectrum of Ga(HDFO)$^+$ (3 pages). Ordering information is given on any current masthead page.

(30) Merbach, A. E. *Pure Appl. Chem.* **1982**, *54*, 1479.
(31) Weast, R. C., Ed. *CRC Handbook of Chemistry and Physics*, 61st ed.; CRC: Boca Raton, FL, 1980; p E5.
(32) Hossain, M. B.; Jalal, M. A. F.; van der Helm, D. *Acta Crystallogr., Sect. C* **1986**, *42*, 1305.
(33) Macura, S.; Ernst, R. R. *J. Mol. Phys.* **1980**, *41*, 95.
(34) Pecoraro, V. L.; Wong, G. B.; Raymond, K. N. *Inorg. Chem.* **1982**, *21*, 2209.